

Recombination distribution and color tuning of multilayer organic light-emitting diode

Chia-Hsun Chen and Hsin-Fei Meng

Citation: *Applied Physics Letters* **86**, 201102 (2005); doi: 10.1063/1.1923759

View online: <http://dx.doi.org/10.1063/1.1923759>

View Table of Contents: <http://scitation.aip.org/content/aip/journal/apl/86/20?ver=pdfcov>

Published by the [AIP Publishing](#)

Articles you may be interested in

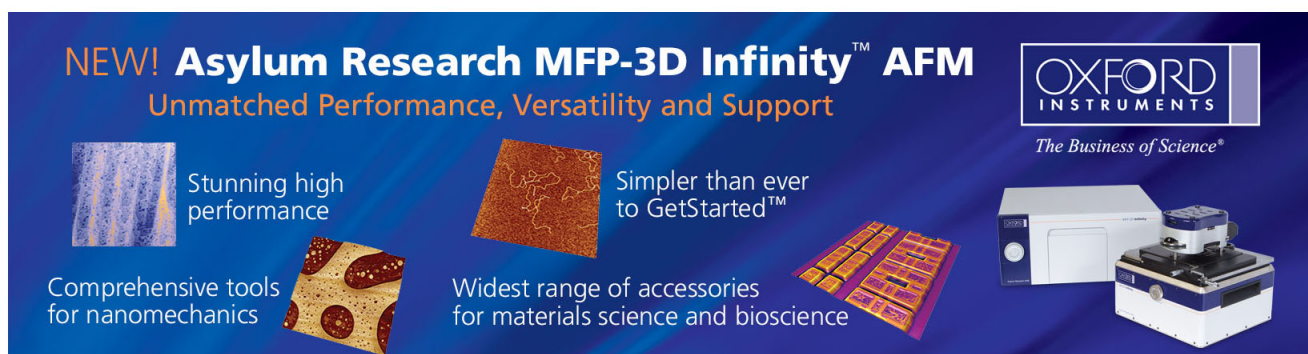
[Relating charge transport and performance in single-layer graded-composition organic light-emitting devices](#)
J. Appl. Phys. **110**, 084515 (2011); 10.1063/1.3653285

[Predictive modeling of the current density and radiative recombination in blue polymer-based light-emitting diodes](#)
J. Appl. Phys. **109**, 064502 (2011); 10.1063/1.3553412

[Direct measurement of the magnetic field effects on carrier mobilities and recombination in tri-\(8-hydroxyquinoline\)-aluminum based light-emitting diodes](#)
Appl. Phys. Lett. **97**, 073301 (2010); 10.1063/1.3478014

[Impedance of space-charge-limited currents in organic light-emitting diodes with double injection and strong recombination](#)
J. Appl. Phys. **100**, 084502 (2006); 10.1063/1.2358302

[Color-tunable multilayer light-emitting diodes based on conjugated polymers](#)
Appl. Phys. Lett. **84**, 1195 (2004); 10.1063/1.1645983

The advertisement features a dark blue background with white and orange text. At the top left, it reads 'NEW! Asylum Research MFP-3D Infinity™ AFM' in large white letters, with 'Unmatched Performance, Versatility and Support' in orange below it. To the right is the Oxford Instruments logo, which includes the text 'OXFORD INSTRUMENTS' and 'The Business of Science®'. Below the main text are four images: a textured surface, a circular pattern, a grid of small squares, and the AFM instrument itself. Each image is accompanied by a short text description: 'Stunning high performance', 'Simpler than ever to GetStarted™', 'Comprehensive tools for nanomechanics', and 'Widest range of accessories for materials science and bioscience'.

Recombination distribution and color tuning of multilayer organic light-emitting diode

Chia-Hsun Chen and Hsin-Fei Meng^{a)}

Institute of Physics, National Chiao Tung University, Hsinchu 300, Taiwan, Republic of China

(Received 6 July 2004; accepted 21 March 2005; published online 9 May 2005)

The recombination distribution of an organic light-emitting diode with multiple emissive layers is studied theoretically. Due to the relatively low electron mobility, the recombination concentrates in the layer next to the cathode. As the voltage increases, the recombination extends to the subsequent layers because the electric field strongly enhances the electron mobility. Assume that the layers are arranged in the order of red, green, blue, and electron blocking from the cathode, the emission color can be continuously tuned by the voltage over a wide range. Taking typical material parameters and emission spectra for the layers, we show that Commission Internationale de L'Eclairage coordinate can move from (0.5,0.5) (orange) to (0.3,0.5) (green) to (0.2,0.3) (blue) as the voltage increases from 3 to 13 V. The ratio between the electron and hole mobilities of the green layer and the electron barrier between green and blue layers is found to be crucial for the wide range of color tunability. © 2005 American Institute of Physics. [DOI: 10.1063/1.1923759]

Organic semiconductors have been used as the emissive materials for efficient light-emitting diodes (LEDs),¹ which cover the whole visible spectra range. It will be highly desirable if one single LED can emit light with a wide range of color, continuously tuned by the applied voltage. Such a tunable LED can be applied in the full-color display, signaling, and illumination. There have been reports of organic voltage-tuning color-tunable LEDs in polymer blends^{2,3} and organic-inorganic composites.^{4,5} Recently, we showed the feasibility of wide-range low-voltage color tuning in polymer LED with multiple emissive layers.⁶ But, without full theoretical understanding of the details, further improvement for each structure is difficult. Multilayer structures have been commonly used for organic LEDs. However, in most cases, there is only one emissive layer while the other layers serve for carrier transport and blocking in order to improve the efficiency. There have been some reports on device simulation for multilayer organic LEDs, which are focused on the quantitative verification of the exciton recombination efficiency improvement owing to the heterojunction.^{7,8} In order to study the color tunability, in this work, we perform detailed calculations on the carrier and recombination distribution of an organic LED with multiple emissive layers. In particular, we calculate the continuous evolution of the recombination distribution as the voltage increases.

Due to the relatively low electron mobility, the recombination concentrates in the material next to the cathode at low voltage. As the voltage increases, the electron mobility increases rapidly with the electric field,⁹ and the electrons moves through the heterojunctions and recombine with the holes in the other layers. The overall results are the continuous shift of the recombination distribution away from the cathode and the change of the ratio among the integrated recombination in each layer. This investigation systematically studies how several device parameters (namely, the junction energy barrier for electron, mobility, and layer thickness) for multilayer organic LEDs influence the recom-

bination current ratio (and therefore the color) among the layers. Based on our results, definite device structures are proposed to have color tuning from orange to green and finally to blue as the voltage increases.

The transport of electrons and holes in the organic device are described by the time dependent continuity equations with a drift-diffusion form for current density, and the Poisson's equation.^{10,11} The electron (hole) mobility, $\mu_n(\mu_p)$, is taken as Poole-Frenkel form, namely $\mu(E) = \mu_0 \exp(\sqrt{E/E_0})$. Carrier recombination is assumed to be bimolecular with the Langevin form, so that the recombination rate is given by $R(x) = e\mu_R[E(x)]n(x)p(x)/\epsilon\epsilon_0$, here μ_R , the effective mobility, is the larger of μ_n or μ_p .¹²⁻¹⁴ These equations are discretized for numerical solution with the Scharfetter-Gummel approach,¹⁵ except for the grid element corresponding to the organic/organic heterojunction. At this junction, discontinuities of the material parameters can lead to discontinuous carrier densities which must be treated as an internal boundary condition in the solution. We take $p(x^-)/p(x^+) = e^{-\Delta\phi_n/k_B T}$ and $n(x^-)/n(x^+) = e^{-\Delta\phi_e/k_B T}$, where $\Delta\phi_n$ ($\Delta\phi_e$) denotes the hole (electron) energy difference in the junction, x^- denotes the grid element on the lower side of the barrier, and x^+ denotes that on the upper side. The recombination current for the red-, green-, and blue-emitting layer is expressed as $J_r^R = \int_0^{x_1} eR(x)dx$, $J_r^G = \int_{x_1}^{x_2} eR(x)dx$, and $J_r^B = \int_{x_2}^{x_3} eR(x)dx$, respectively, where x_1 , x_2 , and x_3 denote the position of the junction between the red and green layers, the green and blue layers, and the blue and electron blocking layers, respectively [referring to Fig. 2(a)]. The relative recombination ratio for other layers to the red layer is $r_{G,B}$ where $r_G = J_r^G/J_r^R$ and $r_B = J_r^B/J_r^R$. They measure the relative exciton recombination efficiency of each layer. Multiplying this ratio by the relative exciton radiation efficiency $\eta_{G,B}$ for the green and blue layer to the red layer produces the relative internal emission efficiency, $R_{G,B} = \eta_{G,B} r_{G,B}$, for each layer.

Because of the high mobility of the holes, the hole distribution is rather uniform throughout the layers, except for the sudden fall and rise at the junctions. On the other hand, the electron density decreases strongly from the cathode typical for the low-mobility space-charge-limited current. It

^{a)} Author to whom correspondence should be addressed; electronic mail: meng@faculty.nctu.edu.tw

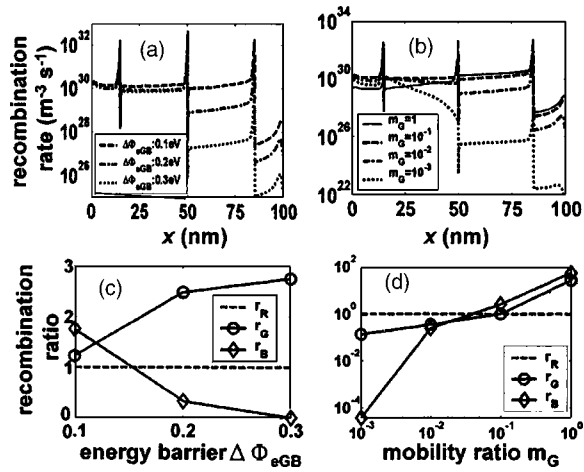


FIG. 1. (a) The recombination rate distribution, $R(x)$, are shown for $\Delta\phi_{eGB}$ equal to 0.1 eV (dashed line), 0.2 eV (dashed-dotted line), and 0.3 eV (dotted line). (b) $R(x)$ is shown for green layer mobility ratio $m_G \equiv \mu_{0eG}/\mu_{0hG}$ equal to 1.0 (solid line), 0.1 (dashed line), 0.01 (dash-dot line), and 0.001 (dotted line). The relative recombination ratio, $r_{G,B}$, as functions of $\Delta\phi_{eGB}$ and m_G are shown in (c) and (d).

is quite difficult for the electrons to not only reach the junction but also jump through it. The recombination distribution, proportional to $n(x)p(x)$, is therefore dominated by the behavior of $n(x)$. Figure 1(a) illustrates how the electron energy barrier between the green and blue layers, $\Delta\phi_{eGB}$, influences the recombination distribution $R(x)$ for the device voltage at 10 V. μ_0 and E_0 for holes are taken as 10^{-11} m²/V s and 4.3×10^6 V/m for each layer.⁹ E_0 for electrons is specified as 1.6×10^6 V/m. μ_0 for electrons is specified as 10^{-12} m²/V s or 2×10^{-12} m²/V s, which will be declared as needed. As $\Delta\phi_{eGB}$ increases from 0.1 eV to 0.3 eV, $R(x)$ for the green layer changes little, but the $R(x)$ for the blue layer decreases dramatically. Figure 1(c) shows the relative recombination ratios, $r_{G,B}$, among the luminescent layers, as functions of the barrier. As $\Delta\phi_{eGB}$ increases from 0.1 eV to 0.3 eV, r_G grows from 1.2 to 2.8 and r_B decays from 1.8 to almost zero. For $\Delta\phi_{eGB} < 0.2$ the recombination in the layers is comparable, such that significant color tuning is possible. As the electron energy barrier between the blue and electron blocking layer $\Delta\phi_{eBE}$ varies between 0.3 eV and 0.6 eV, the relative recombination ratios remain largely unchanged.

Even though the electron mobility is typically several orders of magnitude smaller than the hole mobility, there exist some highly emissive materials for which the mobilities are not so asymmetric.¹⁶ It is therefore important to know how the mobility ratio influences the recombination distribution. Figure 1(b) demonstrates how the zero-field electron mobility of the green layer, μ_{0eG} , determines the $R(x)$ of the device. Define the electron-hole mobility ratio μ_{0eG}/μ_{0hG} as m_G . As m_G decreases from 1.0 to 0.001, the recombination distribution for the green layer shifts to the left. Figure 1(d) shows how m_G influences the recombination ratio $r_{G,B}$. For m_G around 0.1, both r_G and r_B color tuning is expected. Increasing the blue mobility ratio μ_{0eB}/μ_{0hB} will increase r_B approximately linearly, but r_G is suppressed because the faster electron mobility of the blue layer prevents the pile up of electrons in the green layer near the junction between the green and blue layers.

A color-tuning structure should have to tune the color from red to green then to blue as the bias increases. Ideally,

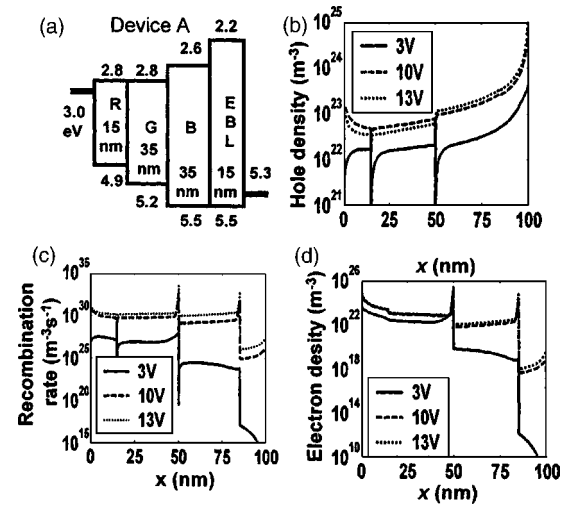


FIG. 2. (a) The structure of Device A. Hole density (b), electron density (c), and recombination rate profile (d) of Device A are shown for various voltages. Electron to hole mobility ratio is taken to be 0.2 for green and 0.1 for other layers. Device B is the same as Device A except that the thicknesses for green and blue layers are changed to 50 nm and 20 nm, respectively, and the mobility ratio is changed to 0.1 for all layers.

the red emission dominates over other colors for low voltage, while the green dominates medium voltage, and the blue increases rapidly for high voltage. Figure 2(a) displays the optimized device structure (Device A). The electron affinity (EA) and ionization potential for each layer are chosen to match the proper energy gap for the color of each layer. In order to raise r_G rapidly with voltage, the EA for the red and green layers are chosen to be the same. However, a 0.2 eV barrier between the green and blue layers will make r_G dominate over the medium voltage range. The 0.4 eV barrier between the blue and electron blocking layer allows r_B to grow rapidly at high voltage. The relative efficiency η_G for Device A is specified as 0.5 and η_B as 1.5. $m_G=0.2$ while the zero-field electron-to-hole mobility ratio for other layers is 0.1. The hole density [Fig. 2(b)] has sudden drops beside each junction. The drops are caused by the efficient carrier “sweep out” across the junction. Once the hole passes the junction, they can hardly “backflow” due to the large hole barrier. As expected, the electron density [Fig. 2(c)] of the blue layer for 3 V is negligible. Even green is small compared with red. As the voltage increases to 10 V, both green and blue becomes comparable to red. To 13 V, blue not only suppresses red but also starts to compete with green. The recombination distribution [Fig. 2(d)] shifts to the anode, reflecting the growth of electron densities in green and blue layers.

To model the color tuning, the Commission Internationale de L'Éclairage (CIE) coordinates as a function of bias is calculated.¹⁷ The LED emission spectrum is $R(\lambda) + R_G G(\lambda) + R_B B(\lambda)$. The normalized luminescence spectra $R(\lambda)$, $G(\lambda)$, and $B(\lambda)$ for the red, green, and blue layers are each taken as a superposition of a main band and a phonon side band, which is redshifted from the main band by an optical phonon energy of 0.17 eV. Both the main and side bands are Gaussians. The strength of the side band is chosen to be one-half of the main band, typical for the luminescent polymers.¹⁸ The peak wavelengths of the main bands for the three colors are $\lambda_R=600$ nm, $\lambda_G=520$ nm, and $\lambda_B=440$ nm. The Gaussian widths of all of the main and side bands are 10 nm. The cavity effect due to the metal cathode on the emission wave-

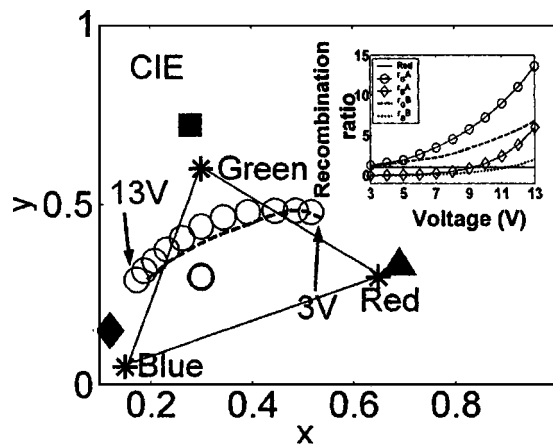


FIG. 3. The trajectories of the CIE coordinates as the voltage changes for Devices A (small open circle) and B (dashed line) are plotted. The three stars are defined by the phosphors of the typical red, green, and blue. The large open circle is white color area. The black triangle is the position of our chosen spectrum for the red layer, the black square is for the green, and the black diamond is for the blue. The inset shows the relative recombination ratio of each layer for Device A (green: open circle; blue: open diamond) and B (green: dashed line; blue: dotted line).

length is also considered. The relation between the wavelength shift $\Delta\lambda$ and the distance d between the exciton and the cathode is found to be approximately $\Delta\lambda=0.33(d-25\text{ nm})$.¹⁹ Because the recombination mostly concentrates near the junctions [Fig. 2(d)], emission comes from a region next to the junction with width equal to the exciton diffusion length. The spectrum depends in principle on the emission region width. However, assuming that the exciton diffusion length is smaller than the layer thickness, we approximate the spectrum by taking the distances for the excitons of each color as the accumulative layer thickness, i.e., $d=15\text{ nm}$ for red, 40 nm for green, and 85 nm for blue. Besides Device A, we also studied Device B with a thicker green layer (50 nm) and a thinner blue layer (20 nm), and the zero-field electron mobilities for each layer are all one order of magnitude smaller than that of the hole. η_G and η_B are the same as Device A. Figure 3 demonstrates the continuous motion of the CIE coordinates for Devices A and B with varying voltage. The stars are the vertices of the CIE triangle defined by the phosphors. The main bands for each color before the cavity shift are indicated as the filled symbols. The trajectories for both A and B go through the orange (0.5 0.5), yellow-green (0.3 0.5), and blue (0.2 0.3) regions. The inset of Fig. 3 shows the relative recombination ratios of Devices A and B from 3 V to 13 V. The relative contributions for the green layers of Devices A and B both start from about 1 and grow gradually with voltage. On the other hand, the contri-

butions for the blue layers of Devices A and B both start from about zero and grow rapidly at high voltage.

In summary, we establish a theoretical model which is able to obtain the carrier and recombination distribution in an organic LED with multiple emissive layers for arbitrary voltage. Due to the asymmetric electron and hole mobility, the recombination ratio in the layers changes continuously with the voltage. Two definite device structures are predicted to have wide-range color tunability from orange to green to blue as the voltage increases from 3 to 13 V.

This work was supported by the National Science Council and the Excellence Project "Semiconducting Polymers for Electroluminescence" of the Ministry of Education of Taiwan, R.O.C.

- ¹R. H. Friend, R. W. Gymer, A. B. Holmes, J. H. Burroughes, R. N. Marks, C. Taliani, D. D. C. Bradley, D. A. Dos Santos, J. L. Brédas, M. Lögdlund, and W. R. Salaneck, *Nature (London)* **397**, 121 (1999).
- ²M. Berggren, O. Inganäs, G. Gustafsson, J. Rasmusson, M. R. Andersson, T. Hjertberg, and O. Wennerstrom, *Nature (London)* **372**, 444 (1994).
- ³O. Inganäs, in *Organic Electroluminescent Materials and Devices*, edited by S. Miyata and H. S. Nalwa (Gordon and Breach, Amsterdam, 1997), p. 147.
- ⁴B. O. Dabbousi, M. G. Bawendi, O. Onitsuka, and K. Yoshino, *Jpn. J. Appl. Phys., Part 2* **66**, 1316 (1995).
- ⁵V. L. Colvin, M. C. Schlamp, and A. P. Alivisatos, *Nature (London)* **370**, 354 (1994).
- ⁶C. C. Huang, H. F. Meng, G. K. Ho, C. H. Chen, C. S. Hsu, J. H. Huang, S. F. Horng, B. X. Chen, and L. C. Chen, *Appl. Phys. Lett.* **84**, 1195 (2004).
- ⁷B. K. Crone, P. S. Davids, I. H. Campbell, and D. L. Smith, *J. Appl. Phys.* **87**, 1974 (2000).
- ⁸B. Ruhstaller, S. A. Carter, S. Barth, H. Riel, and J. C. Scott, *J. Appl. Phys.* **89**, 4575 (2001).
- ⁹L. Bozano, S. A. Carter, J. C. Scott, G. G. Malliaras, and P. J. Brock, *Appl. Phys. Lett.* **74**, 1132 (1999).
- ¹⁰P. S. Davids, I. H. Campbell, and D. L. Smith, *J. Appl. Phys.* **82**, 6319 (1997).
- ¹¹B. K. Crone, P. S. Davids, I. H. Campbell, and S. L. Smith, *J. Appl. Phys.* **84**, 833 (1998).
- ¹²V. N. Abakumov, V. I. Perel, and I. N. Yassievich, in *Nonradiative Recombination in Semiconductors* (North-Holland, Amsterdam, 1991), p. 108.
- ¹³U. Albrecht and H. Bässler, *Phys. Status Solidi B* **191**, 455 (1995).
- ¹⁴P. W. M. Blom, M. J. M. de Jong, and S. Breedijk, *Appl. Phys. Lett.* **71**, 930 (1997).
- ¹⁵D. L. Scharfetter and H. K. Gummel, *IEEE Trans. Electron Devices* **16**, 64 (1969).
- ¹⁶Z. G. Yu, D. L. Smith, A. Saxena, R. L. Martin, and A. R. Bishop, *Phys. Rev. Lett.* **84**, 721 (2000).
- ¹⁷C. L. Novak and S. A. Shafer, in *Color: Physics-Based Vision, Principles and Practice*, edited by G. E. Healey, S. A. Shafer, and L. B. Wolff (Jones and Bartlett, Boston, 1992), p. 1.
- ¹⁸H. F. Meng and C. H. Chang, *Phys. Rev. B* **60**, 14242 (1999).
- ¹⁹V. Bulovic, V. B. Khalfin, G. Gu, P. E. Burrows, D. Z. Garbuzov, and S. R. Forrest, *Phys. Rev. B* **58**, 3730 (1998).